© Universiti Tun Hussein Onn Malaysia Publisher's Office

IJIE

http://penerbit.uthm.edu.my/ojs/index.php/ijie
ISSN : 2229-838X e-ISSN : 2600-7916

The International Journal of Integrated Engineering

Numerical Investigation on Reduced Moment Resistance and Increased Reinforcement Spacing in Reinforced Concrete Wall Subjected to Blast Load

M. A. Seman[1*], S. M. Syed Mohsin[2], A. M. A. Zaidi[3], Z. M. Jaini[4]

[1]Department of Civil Engineering, College of Engineering
Universiti Malaysia Pahang, Gambang, 26300, MALAYSIA

[2]Faculty of Civil Engineering Technology,
Universiti Malaysia Pahang, Gambang, 26300, MALAYSIA

[3]Department of Mechanical Engineering
Universiti Pertahanan Nasional Malaysia, Sungai Buloh, 57000, MALAYSIA

[4]Faculty of Civil Engineering and Built Environment,
Universiti Tun Hussein Onn Malaysia, Batu Pahat, 86400, MALAYSIA

DOI: https://doi.org/10.30880/ijie.2022.14.01.032
Received 01 October 2021; Accepted 23 December 2021; Available online 07 March 2022

Abstract: Numerical investigation becomes a highly demanding tool for the best design in engineering. With one validated numerical result available, further investigation is possible to conduct. Especially, for the expensive and limited access for civilian to conduct the test like a blast experiment. With the capability of Arbitrary Lagrange Euler (ALE) solver coupling approach between structure and air in AUTODYN, a detail three-dimensional assessment for RC wall on reduced moment resistance and increased reinforcement spacing are conducted. The RC wall has a cross-sectional dimension of 1829 mm x 1219 mm with wall thickness of 305 mm thickness of strip footing. It is subjected to 13.61 kg Trinitrotoluene (TNT) explosive at 1.21 m standoff distance from the centre. The numerical blast impact on RC wall indicated, although the horizontal and vertical flexural reinforcements are reduced from one of the simulated RC walls, it is capable of demonstrating an equivalent strength to the RC wall tested in the experiment.

Keywords: Reinforced concrete, wall, blast, simulation, AUTODYN

1. Introduction

Generally, plain concrete is recognised to have a comparatively good blast resistance when compared to other construction materials. However, plain concrete with a higher strength, on the other hand, would result in a brittle collapse when compared to ordinary concrete. As a result, when the correct quantity of steel reinforcement is combined with the suitable concrete strength, the outcome is ductile concrete, which limits structural damage in RC structural elements. To study the damage caused by blast loads in various scopes of work, a series of experimental and numerical studies have been carried out. The research revealed the potential for several methods of improving the strength of ordinary reinforced concrete structures, such as retrofitting the concrete material with steel fibre [1-4]; replaced normal strength steel with enamel coated steel [5] or retrofitted the structure with a new material like aluminium foam [6]. However, some experimental tests indicate inconsistent results or even worse than ordinary reinforced concrete when it comes to strengthening reinforced concrete. For example, when glass fibre reinforced polymer was used to retrofit reinforced panels, it was discovered that in some situations the retrofitted panels outperformed the unretrofitted panels, but in other cases the converse was true [7]. In the case of carbon fibre reinforced polymer plate utilised to retrofit on compression and tension side of the panel, it was discovered that the post-impact scabbing hole in the retrofitted panel was substantially

*Corresponding author: mazlanseman@ump.edu.my

bigger than the unretrofitted panel [8]. In addition, when a structure was subjected to a blast load, the use of high-strength concrete did not significantly improve the performance [9]. Although the reinforced concrete slab panel may be simplified as an RC wall with specified restrain either experimentally or numerically, the real construction is necessary to assess the reinforced concrete wall with strip footing. This is due to the fact that the primary steel in the wall must be linked into its base when using the wall foundation. As to date, inverted T-shaped RC walls, L-shaped RC walls, RC column-beam connections, and RC columns have been published academically for various purposes, including the different steel reinforcement arrangements, the performance of various steel reinforcement materials used in RC structures, the effectiveness of high-strength steel fibres and high compressive strength aggregate concrete, dynamic response and damage characteristics, and the influence of column width and height [10-14]. For the T-shape RC wall, the horizontal steel reinforcement tied-outside on the vertical steel reinforcement and the vertical steel reinforcement hooked-in into the base are the appropriate steel reinforcement arrangements with its base when exposed to blast load [10].

2. Numerical Blast

In this study, the appropriate steel reinforcement configuration for RC-WTB wall subjected to blast load in the experimental [10] selected. The cross-section of the RC-WTB wall is 1828.8 mm x 1219 mm, with a wall thickness of 164.9 mm and a footing thickness of 304.8 mm. The vertical flexural reinforcement is 16 mm, and the horizontal flexural reinforcement is 10 mm, both spaced at 139.7 mm (5.5 inches) in the main bending plane and 152.4 mm (6 inches) in the minor bending plane on these walls. Steel reinforcement and concrete have respective strengths of 460 N/mm2 and 35 N/mm2 [10]. The cutting section of the RC-WTB is shown in Fig. 1, together with the location of strain and displacement gauges on the main steel reinforcement. Fig. 2 and Fig. 3 indicate where the strain and displacement gauges for the RC-WTB1 and RC-WTB2 are located, respectively. The detail of the reinforcement spacing for reduced moment resistance and increased reinforcement spacing is detail in Table 1. The RC walls were meshed with a fine hexahedral mesh size of 10 mm [21] and subjected to a 10.16 kg Plastic Explosives (PE4) at a standoff distance of 1,219 mm (4 ft.) from the wall centre.

To get an accurate prediction of concrete behaviour under blast loads, a suitable model that reflects concrete material behaviour characteristics at high strain rates is required. For this investigation, Riedel, Hiermayer, and Thoma (RHT) [22] created a material model. The RHT concrete model is an advanced plasticity model for brittle materials. It's very useful for simulating the dynamic loading of concrete. The model includes pressure hardening, strain hardening, strain rate hardening, third invariant dependence for compressive and tensile loads, as well as a damage model for strain softening. This model also uses the p-α equation of state (EOS) to depict real thermodynamic behaviour under high stress, and it gives a very thorough explanation of compaction behaviour under low stress [23]. The material data for CONC-35MPA [24] is used in this simulation, and the modifications are performed based on experimental data [10]. For the crack failure of the RC wall structure, the strain limit on vertical direction is controlled between -0.0035 and 0.00219. The Johnson-Cook (JC) material model was utilised for steel reinforcement [25]. This model depicts the strength of a material, generally metal, that has been exposed to a significant strain, high strain rates, and high temperature. The material data for STEEL 4340 [24] is used in this simulation, and the modifications are performed based on experimental data [10]. The ALE is a numerical approach for analysing the interface between air and structure. Different parts of the solver, such as structure, fluids, and gases, may be represented concurrently utilising the Lagrange and Euler approach. These several solvers then coupled together in space and time. The ideal gas EOS is used to simulate air, whereas the Jones-Wilkins-Lee (JWL) EOS is used to model high explosives like TNT [24]. To depict the explosive's initial explosion and blast wave propagation in AUTODYN, an axially symmetric wedge shape is utilised. The predicted charge circle for 13.61 kg (30 lbs.) of TNT material model fills the 1 m wedge, with the air material filling the remaining. The wedge, which is made up of blast pressure history, is created before applying the explosion effect to a 3D model using AUTODYN's remap function [26].

In the simulation, the RC wall is placed on the ground as shown in Fig. 4. The displacement gauges were set on the left and right wall bases, and fixed end support was used to attach at five ground surfaces. For friction coefficient, dynamic coefficient, and dynamic constant, the standard frictional contact surface between the wall base and the ground is 0.3, 0.5, and 1.0, respectively. The standard material model for ground in the AUTODYN material library was initially utilised to estimate the ground shock in the numerical simulation. However, in the computational study of the ground shock with large strain, the modified and calibrated material provided by De [28] was used to investigate the appropriate effect of the explosion to mimic the impact of the blast test conducted. Fig. 5 shows 1 meter blast overpressure vectors mapped in the air domain. The pressure gauges placed at 1.219 m (4 ft.) and 5.4864 m (18 ft.) away from the centre of charge weight on each side. Also, installed on the front surface of the wall to analyse how the pressure profile influenced the RC wall and compare with previous study [26].

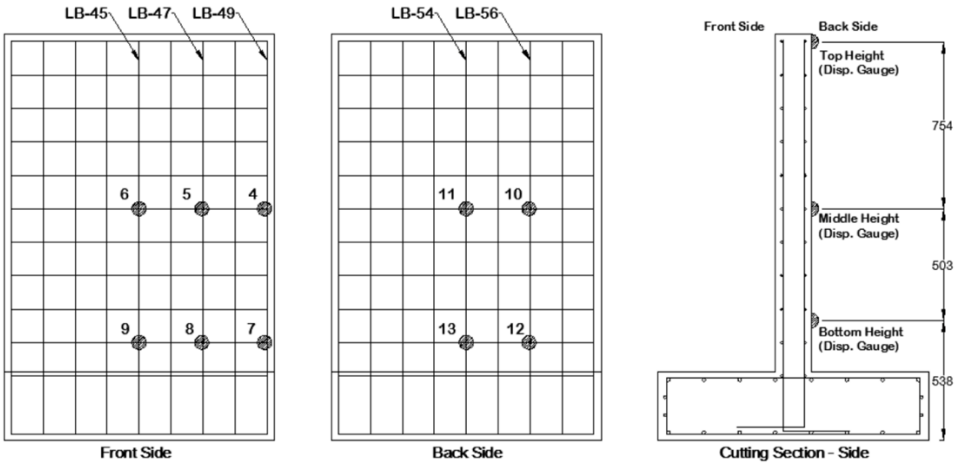

Fig. 1 - Strain and displacement gauges (RC-WTB)

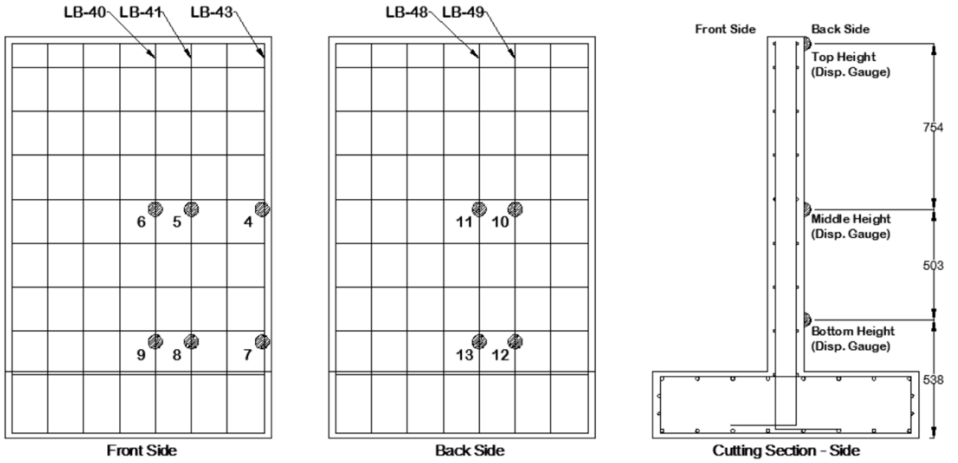

Fig. 2 - Strain and displacement gauges (RC-WTB1)

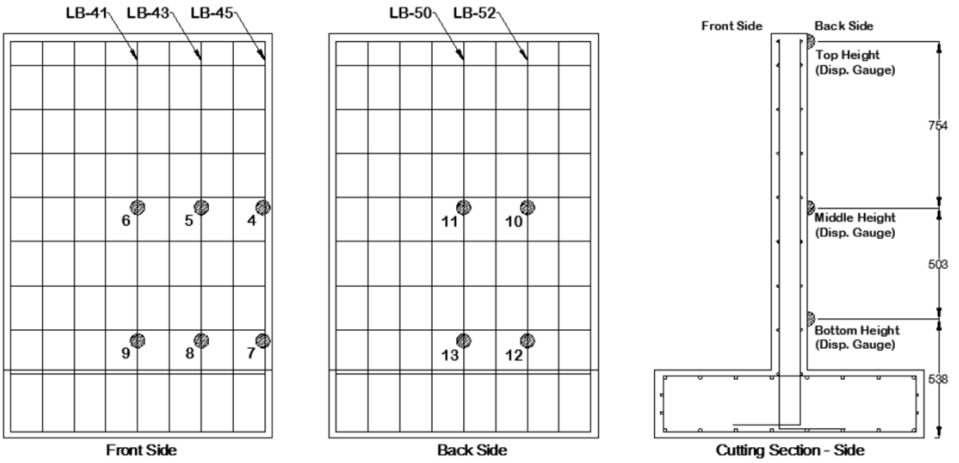

Fig. 3 - Strain and displacement gauges (RC-WTB2)

Table 1 - Detail of steel reinforcement spacing

RC Wall	Horizontal flexural spacing (mm)	Vertical flexural spacing (mm)
(a) RC-WTB	1	2
(b) RC-WTB1	3	4
(c) RC-WTB2	5	6

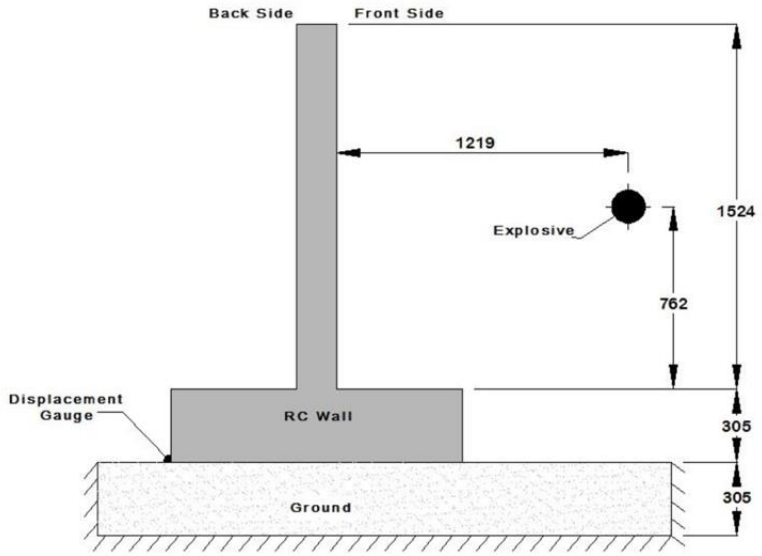

Fig. 4 - Setup for the blast simulation (in mm)

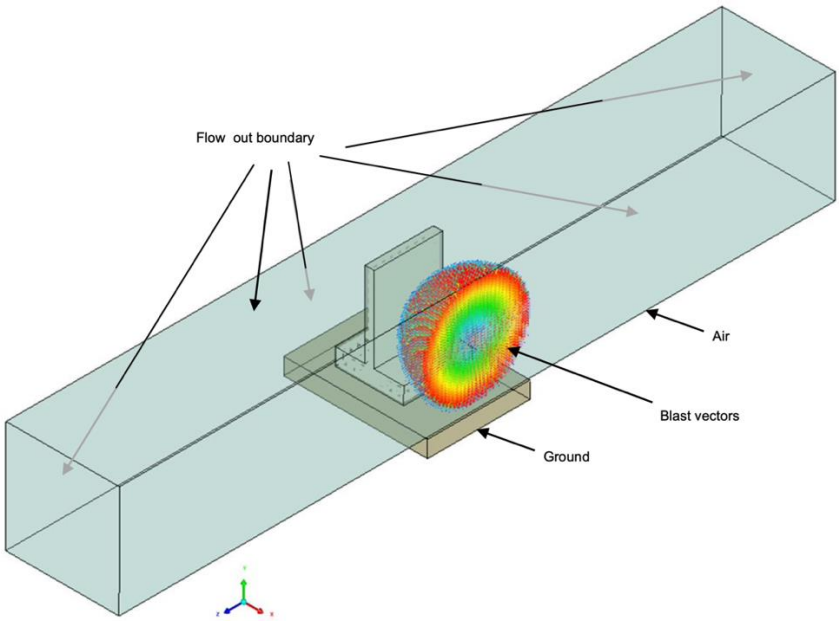

Fig. 5 - One-meter blast overpressure vectors mapped in air volume

3. Numerical Blast Impact Assessment

The blast overpressure-time history profile on all RC wall surfaces is nearly identical to that seen in earlier investigations. [26]. Due to the explosion at the moment of 0.24 msec on the bottom height of the front side of the wall, the overpressure reached a maximum of 13,949 kPa. Conversely, at 0.14 msec and 0.19 msec, the overpressure at the middle and top heights reaches 10,509 kPa and 9,262 kPa, respectively. It can be observed that the overpressure decreases to its ambient value in less than 3 msec following the explosion. The RC walls are pushed backward as a result of the

overpressure. The RC-RTB wall is pushed backward by 60 mm from the position before the impact, as illustrated in Fig. 6 at 39 msec, according to the gauge placed at the RC-WTB wall base. The displacement of the wall base should be 98 mm at 60 msec. The actual displacement based on the blast test result for RC-WTB was 120 mm [10]. As a consequence, the numerical result in terms of displacement distance seems to be reliable. The time history recorded in the numerical simulation shows that the RC-WTB displacement is smaller than the RC-WTB1 and RC-WTB2 displacements by an average of 2 mm and 1 mm, respectively. Both walls displaced at a distance of 54 mm after 35 msec, whereas the RC-WTB displaced at 53 mm. Further observation is made on the location of plastic hinges as shown in Fig. 7; the second plastic hinge for both RC-WTB1 and RC-WTB2 appeared at the bottom height (section) after 0.50 msec. However, as compared to RC-WTB wall at the same time of 0.50 msec the second plastic hinge already occurred.

The comparisons of the strain-time history for RC-WTB, RC-WTB1, and RC- WTB2 are given in Fig. 8 and Fig. 9. Due to less moment resistance i.e less number of vertical flexural reinforcement in RC-WTB1 compared to others, the strain gauge locations are not identical except for Gauge 4 and 7. It is observed through strain Gauge 4 and 7 that a slightly longer time is needed for it to get back to the same strain value of 0.00015 and 0.00017, respectively with an average difference of 4 msec. For Gauge 4, the higher strain magnitude was recorded for the RC-WTB2, followed by RC- WTB, whereas the lowest strain was recorded for the RC-WTB2 with values of 0.00033, 0.00029 and 0.00028, respectively. However, the higher magnitude observed for Gauge 7 is in the following order: RC-WTB1, RC-WTB2 and RC-WTB with strain values of 0.00080, 0.00076, and 0.00072, respectively. For the strain gauges placed at the same location for RC-WTB and RC-WTB2, it is noticeable that the moment resistance is similar, but less horizontal flexural reinforcement is designed for RC-WTB2.

A general observation can be made from the strain-time history pattern. The strain fluctuates in the first 13 msec with an average time of 1.63 msec before attaining maximum strain. According to the overpressure-time history, the average time for the maximum pressure or blast wave to impact the surface is 0.25 msec. The time difference is due to the time of the compressive stress wave required to propagate in the wall until it reaches the back side of the wall. It can be seen that in the duration, another compressive stress wave reflection occurred in the wall for a few times until the remaining stress wave got weaker. The structure can contain the wall core without further damaging it. It appears that beyond 13 msec, the strains gradually increase to the maximum magnitude before gradually decreasing due to structural resistance. It can be deduced through this gradual increase and decrease of strain-time history patterns and cracks that transpire for RC-WTB as explained earlier that, lesser cracks would occur if the actual blast test was conducted for RC-WTB1.

As illustrated in the strain indicator at the instant of 31.62 msec of the numerical simulation in Fig. 10, it can be observed that the amount of horizontal cracks at the back side of RC-WTB1 and RC-WTB2 are considerably lesser than that of RC-WTB. This is due to the lesser amount of horizontal flexural reinforcement used in both the walls as compared to the RC-WTB. As reported earlier, the strain concentration for RC- WTB1 is much higher than RC-WTB2 and RC-WTB at the location of strain failure i.e., the cracks that follow the horizontal flexural reinforcement grid in the RC wall on the front side. However, in general, the amount of scattered strain indicator is rather similar as shown in Fig. 7. Therefore, it is predicted that no cracks will appear on the front side for RC-WTB1 and RC-WTB2 walls as well if the actual blast test was conducted.

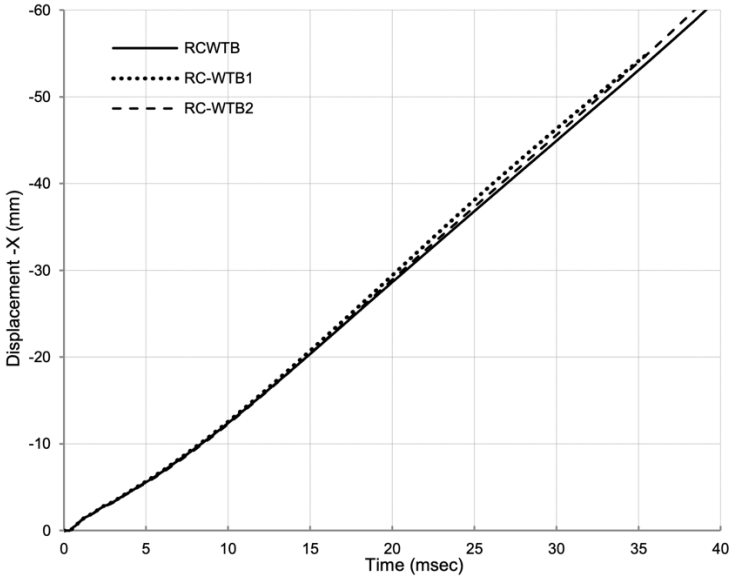

Fig. 6 - Comparison of wall base movement from the original location

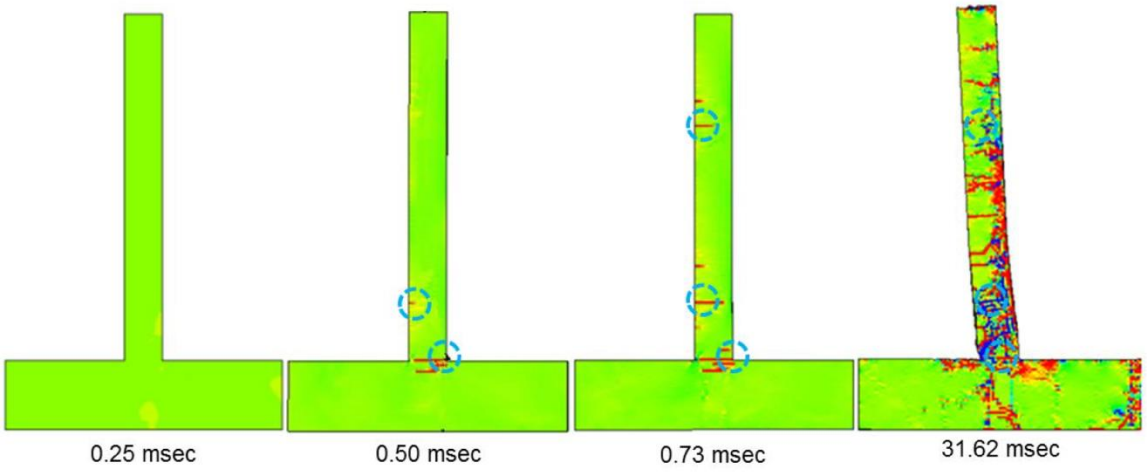

(a)

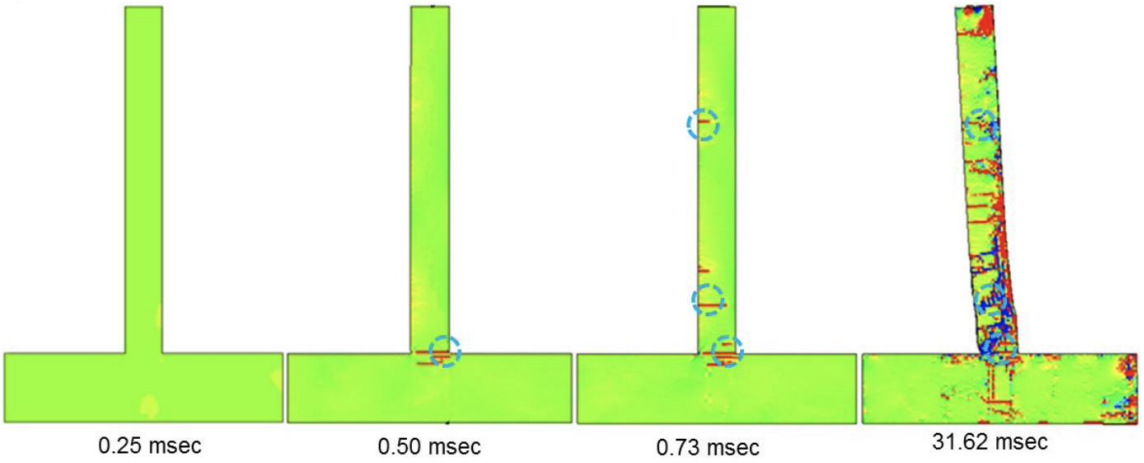

(b)

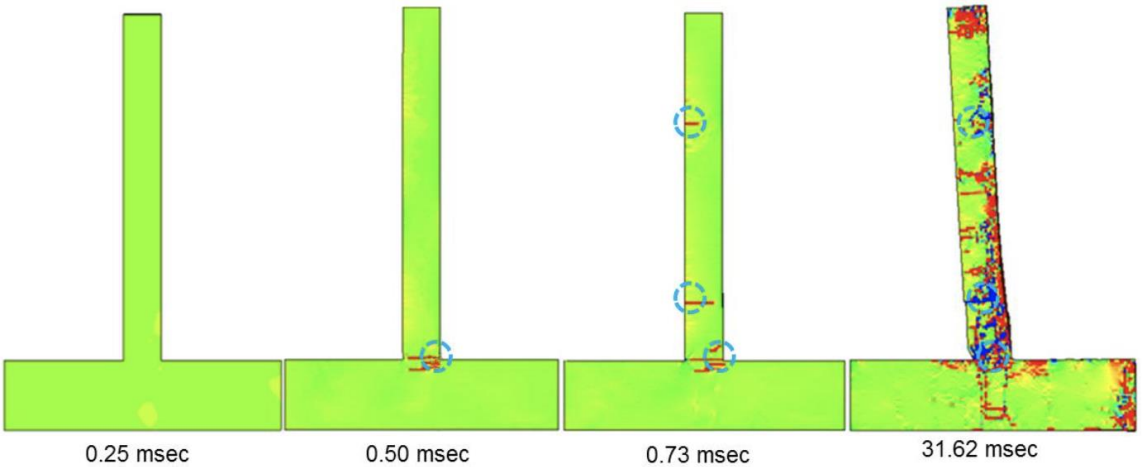

(c)

Fig. 7 - Progression of plastic hinges (a) RC-WTB; (b) RC-WTB1; (c) RC-WTB2

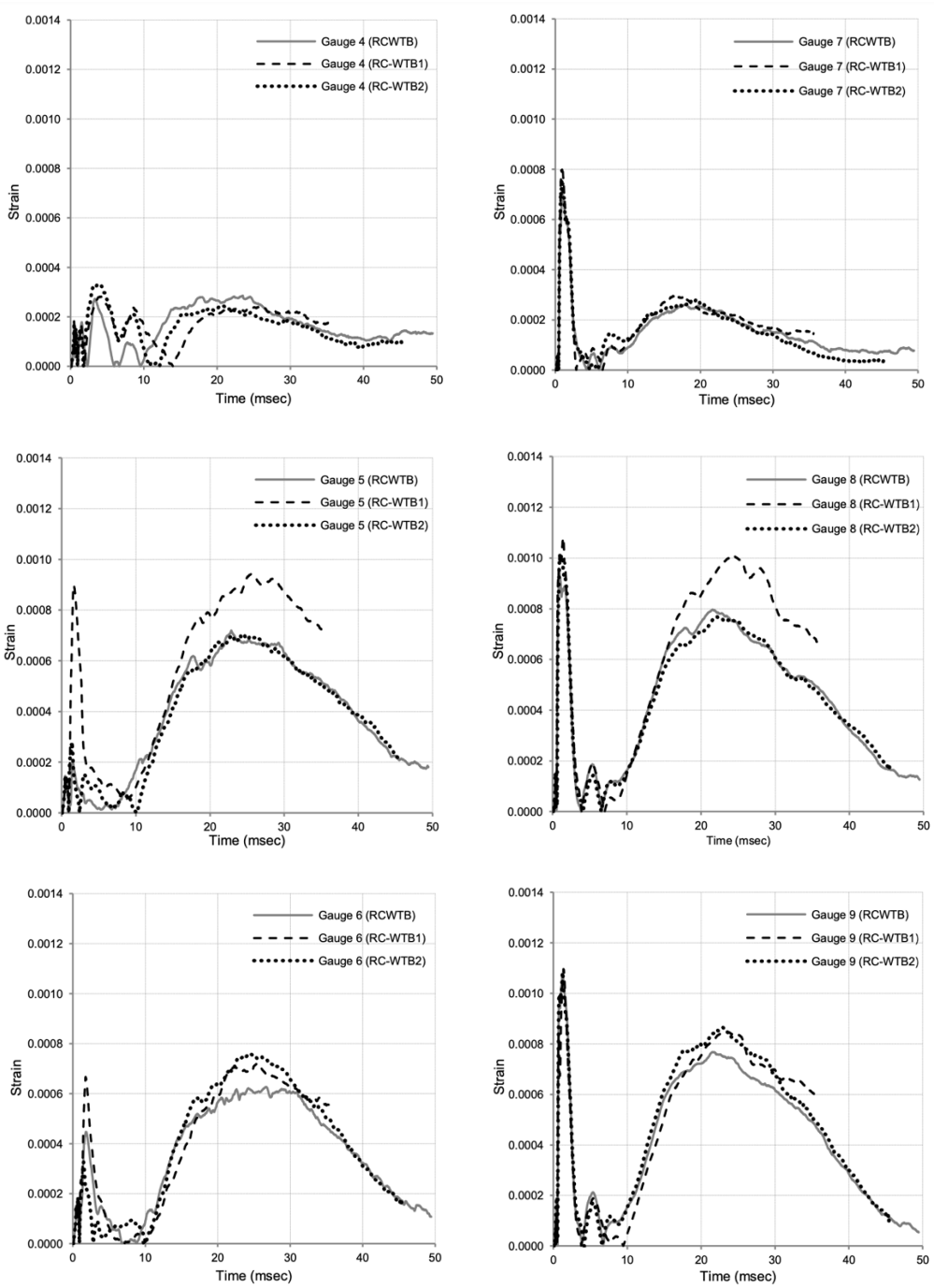

Fig. 8 - Strain-time history at the front side (RC-WTB, B1 and B2)

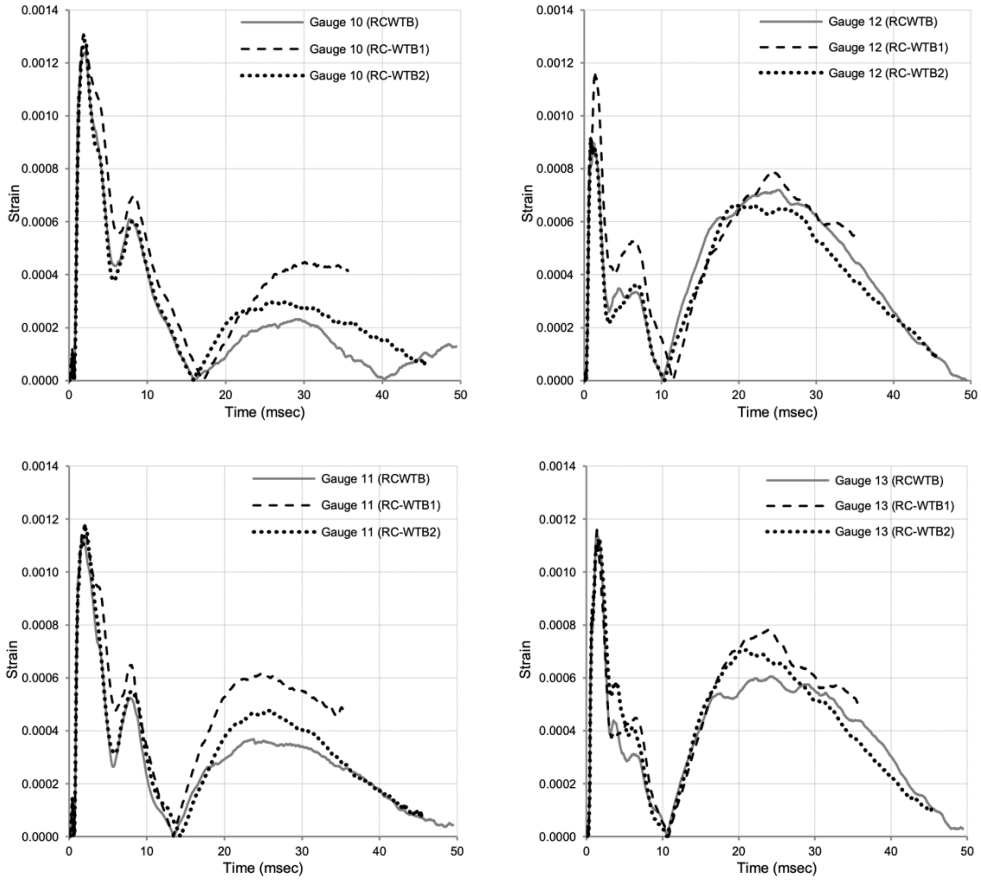

Fig. 9 - Strain-time history at the back side (RC-WTB, B1 and B2)

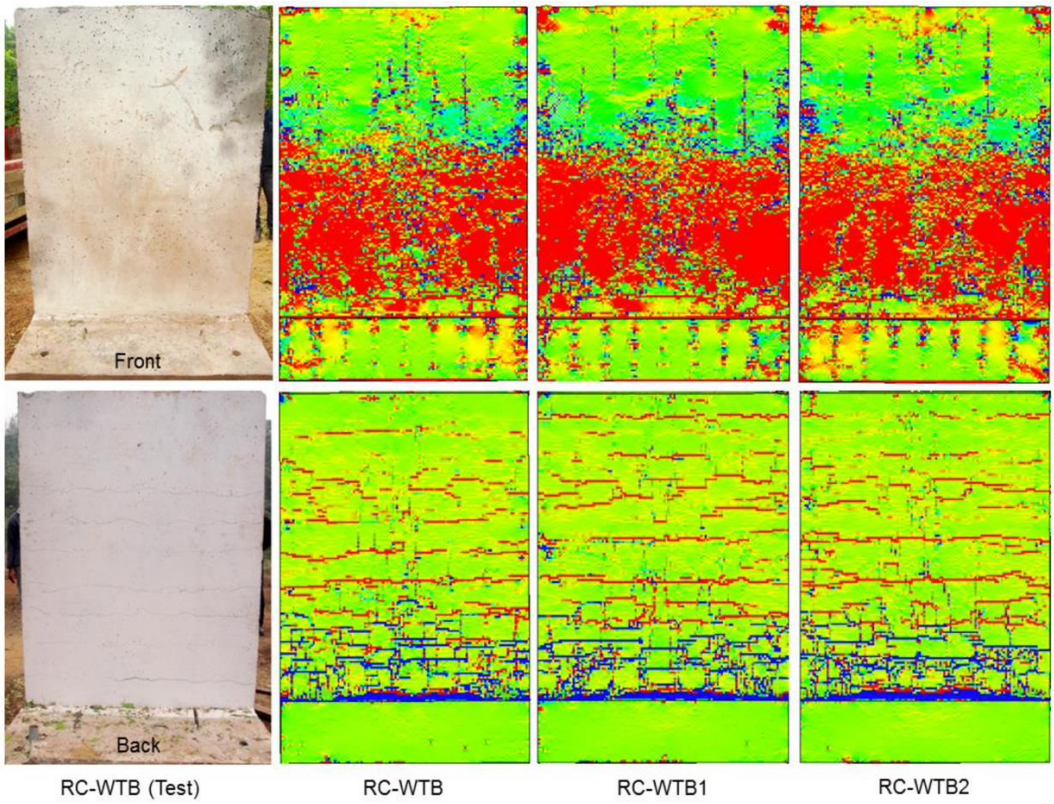

Fig. 10 - Blast test and strain failure at 31.62 msec

4. Summary

Through the numerical validation, it is demonstrated that acceptable results were attained in particular with regards the strain pattern and wall displacement against the experimental works carried out. It was further shown through the numerical optimisation that RC-WTB1 is capable of demonstrating an equivalent strength akin to RC-WTB although the horizontal and vertical flexural reinforcements are reduced. In addition, the RC-WTB1 indicated desirable properties in absorbing the blast wave and the subsequent compressive stress wave.

Acknowledgement

The authors would like to acknowledge the Ministry of Higher Education Malaysia and Universiti Malaysia Pahang, which collectively funded this project in the form of research grants (RDU1903146).

References

[1] Ohtsu, M., Uddin, F. A. K. M., Tong, W., & Murakami, K. (2007). Dynamics of spall failure in fiber reinforced concrete due to blasting. Construction Building Material, 21(3) 511-518.
[2] Zhou, X. Q., & Hao, H. (2008). Numerical prediction of reinforced concrete exterior wall response to blast loading. Advance Structure Engineering, 11(4) 355-365.
[3] Wu, C., Oehlers, D. J., Rebentrost, M., Leach, J., & Whittaker, A. S. (2009). Blast testing of ultra high-performance fibre and FRP-retrofitted concrete slabs. Engineering Structures, 31(9) 2060-2069.
[4] Yusof, M. A., Mohamad Nor, N., Ismail, A., Mohd Sohaimi, R., Nik Daud, N. G., Peng, N. C., & Fauzi, M. Z. M. (2010). Field blast testing using high speed data acquisition system for hybrid steel fiber reinforced concrete panel. European Journal of Scientific Research, 44(4)585-595.
[5] Yan, D., Chen, G., Baird, J., Yin, H., & Koenigstein, M. (2011). Blast test of full-size wall barriers reinforced with enamel-coated steel rebar. Structures Congress, ASCE, 1538-1551.
[6] Schenker, A., Anteby, I., Gal, E., Kivity, Y., Nizri, E., Sadot, O., Michaelis, R., Levintant, O., & Ben-dor, G. (2008) Full-scale field tests of concrete slabs subjected to blast loads, International Journal of Impact Engineering, 35, 184-198.
[7] Ghani Razaqpur, A., Tolba, A., & Contestabile, E. (2007). Blast loading response of reinforced concrete panels reinforced with externally bonded GFRP laminates. Composites Part B: Engineering, 38 (5-6) 535-546.
[8] Wu, C., Nurwidayati, R., & Oehlers, D. J. (2009) Fragmentation from spallation of RC slabs due to airblast loads, International Journal of Impact Engineering, 36(12) 1371-1376.
[9] Morales-Alonson, G., Cendon, D. A., Galvez, F., Erice, B., & Sanchez-Galvez, V. (2011). Blast response analysis of reinforced concrete slabs: Experimental procedure and numerical simulation. Journal of Applied Mechanics, 78,1-12.
[10] Seman, M. A., Syed Mohsin, S. M., Zaidi, A. M. A., Koslan, M. F. S., & Jaini, Z. M. (2021). Experimental of inverted-T shape reinforced concrete wall subjected to blast load. Key Engineering Materials, 879, 254-262.
[11] Yan, D., Chen, G., Baird, J., Yin, H., & Koenigstein, M. (2011). Blast test of full-size wall barriers reinforced with enamel-coated steel rebar. Proceedings of the Structure Congress, pp. 1538-1551.
[12] Radek, H., Marek, F., & Josef, F. (2016). Influence of barrier material and barrier shape on blast mitigation. Construction and Building Material, 120, 54-64.
[13] Chao, L. S., Dan, L., & Bo, Y. (2019). Experimental study and numerical simulation on damage assessment of reinforced concrete beams. International Journal of Impact Engineering, 132, 103323.
[14] Dua, A., Braimah, A., & Kumar, M. (2020). Experimental and numerical investigation of rectangular reinforced concrete T columns under contact explosion effects. Engineering Structure, 205, 109891.
[15] Castedo, R., Segarra, P., Alanon, A., Lopez, L.M., Santos, A.P., & Sanchidrian, J.A. (2015). Air blast resistance of full-scale slabs with different compositions: Numerical modeling and field validation. International Journal of Impact Engineering, 86, 1419-1426.
[16] Thiagarajan, G., Kadambi, A.V., Robert, S., & Johnson, C. F. (2015). Experimental and finite element analysis of doubly reinforced concrete wall subjected to blast loads. International Journal of Impact Engineering, 75, 162–173.
[17] Kong, X., Qi, X., Gu, Y., Lawan, I. A., & Qu, Y. (2018) Numerical evaluation of blast resistance of RC slab strengthened with AFRP. Construction and Building Materials, 178, 244-253.
[18] Jin, M., Hao, Y., & Hao, H. (2019) Numerical study of fence type blast walls for blast load mitigation. International Journal of Impact Engineering, 131, 238-255.
[19] Zhao, C., Wang, Q., Huang, X., & Mo, Y. L. (2019). Blast resistance of small-scale RCS in experimental test and numerical T analysis. Engineering Structures, 199, 109610.
[20] Kumar, V., Kartik, K. V., & Iqbal, M. A. (2020). Experimental and numerical investigation of reinforced concrete slabs under T blast loading. Engineering Structures, 206, 110125.
[21] Seman, M. A., Syed Mohsin, S. M., Zaidi, A. M. A., & Jaini, Z. M. (2021). Numerical investigation of steel reinforced concrete wall subjected to blast. IOP Conference Series: Earth and Environmental Science, 682, 012039

[22] Riedel, W., Thoma, K., Hiermaier, S. (1999). Penetration of reinforced concrete by BETA-B-500 – Numerical analysis using a new macroscopic concrete model for hydrocodes. Proceeding of 9th International Symposium on Interaction of the Effect of Munitions with Structures, 315-322.
[23] Herrmann, W. (1969). Constitutive equation for the dynamic compaction of ductile porous materials. Journal of Applied Physics, 40, 2490-2499.
[24] ANSYS AUTODYN (2020). User's manual, Release 17, ANSYS Inc.
[25] Johnson, G. R., Cook, W. H. (1983). A constitutive model and data for metals subjected to large strains, high strain rates and high temperatures. Proceeding of the 7th International Symposium on Ballistic, 541-547.
[26] Seman, M. A., Syed Mohsin, S. M., Jaini, Z. M. (2019). Numerical analysis of blast pressure distribution on RC wall surface. International Journal of Recent Technology and Engineering, 8-3S3, 524-531.